years) who underwent ultrasound-guided liver biopsy between 2008 and 2010 for the diagnosis of NAFLD. They were patients who agreed with liver biopsy among 268 patients who had admitted to our clinics and had been advised to receive liver biopsy because of the clinical diagnosis of NAFLD during the study period. Liver biopsy was performed to examine the presence of NASH and to confirm the diagnosis. Patients were clinically diagnosed with NAFLD prior to biopsy based on the following criteria: (i) persistent abnormal liver function tests for more than 3 months, (ii) ultrasonographic images showing steatosis, (iii) no evidence of alcohol abuse, and (iv) exclusion of other liver diseases and other known causes of steatosis based on the results of specific clinical, biochemical, or imaging studies. The ultrasonographic findings of steatosis were based on established criteria such as hepatorenal echo contrast, liver brightness, deep attenuation, and vascular blurring (Hamaguchi et al. 2007). The first two criteria were used as definitive criteria, while the latter two criteria were taken into account as needed. All patients were confirmed not to have chronic viral hepatitis with negative results for hepatitis B virus (HBV) surface antigen, HBV DNA, hepatitis C virus (HCV) antibody, and HCV RNA. No patients were diagnosed as having autoimmune hepatitis, primary biliary cirrhosis, or other liver diseases.

All patients underwent ultrasonography-guided fine needle liver biopsy using a 17G biopsy needle. NAFLD was pathologically diagnosed based on pathologic findings in the biopsied liver specimens. The liver biopsy specimens were stained with hematoxylin and eosin, Masson's trichrome, and periodic-acid Schiff stains and then examined by experienced pathologists. The liver specimens were categorized into types 1–4 pathologically based on Matteoni classification (Matteoni et al. 1999), and types 3 and 4 were defined as NASH. Patologic evaluations were performed by two pathologists independently.

The study protocol was in compliance with the Helsinki Declaration and was approved by the institutional review board of Ogaki Municipal Hospital. All patients provided written informed consent for the use of their clinical data and the analyses of biopsy specimens and serum samples.

RNA extraction and real-time PCR for gene expression analyses

Liver biopsy specimens were stored in Ambion RNAlater solution (Life Technologies, Carlsbad, CA, USA) at –80°C until RNA extraction. Total RNA was extracted using the mirVana miRNA isolatidon kit (Life Technologies) according to the manufacturer's instructions.

cDNA was synthesized using the Transcriptor High Fidelity cDNA Synthesis Kit (Roche, Basel, Switzerland). Total RNA (2 mg) in 10.4 μL of nuclease-free water was added to 1 mL of 50 mM random hexamer. The denaturing reaction was performed for 10 min at 65°C. The denatured RNA mixture was added to 4 mL of 5× reverse transcriptase buffer, 2 mL of 10 mM dNTP, 0.5 mL of 40 U/mL RNase inhibitor, and 1.1 mL of reverse transcriptase (FastStart Universal SYBR Green Master, Roche) in a total volume of 20 mL. The reaction ran for 30 min at 50°C (cDNA synthesis), and 5 min at 85°C (enzyme denaturation). All reactions were run in triplicate. The Chromo4 detector (Bio-Rad, Hercules, CA, USA) was used to detect mRNA expression. The primer sequences are follows: TIMP1: 5′-cttggcttctgcactgatgg-3′ (sense), 5′-acgctggtataaggtggtct-3′ (antisense); TIMP2: 5′-agtggactctggaaacgaca-3′ (sense); 5′-tctctgtgacccagtccatc-3′ (antisense); MMP2: 5′- aacgccgatggggagtactg-3′ (sense); 5′-cagggctgtccttcagcgtt-3′ (antisense); MMP13: 5′-gaggctccgagaaatgcagt-3′ (sense); 5′-atgccatcgtgaagtctggt-3′ (antisense); and β-actin: 5′-ccactggcatcgtgatggac-3′ (sense), 5′-tcattgccaatggtgatgacct-3′ (antisense). Assays were performed in triplicate, and the expression levels of target genes were normalized to the expression of the β-actin gene as quantified using real-time quantitative PCR as an internal control.

Measurement of serum levels of fibrosis-associated proteins

Serum levels of TIMP1, MMP2, and hyaluronic acid were measured in stored fasting serum samples that had been obtained at the time of liver biopsy. Serum TIMP1 levels were measured by enzyme immunoassay (hTIMP-1 kit, Daiichi Fine Chemical, Toyama, Japan). Serum MMP2 levels were measured by enzyme immunoassay (hMMP-2 Activity Assay System, GE Healthcare Japan, Tokyo, Japan). Serum hyaluronic acid was measured by the latex agglutination method (Hyaluronic acid LT, Wako Pure Chemical Industries, Osaka, Japan).

Statistical analysis

Quantitative values are expressed as means ± SD. Between-group differences were analyzed by the chi-square test. Differences in quantitative values between two groups were analyzed by the Mann–Whitney *U* test. Correlation between liver tissue mRNA and serum levels of TIMP1 and MMP2 were evaluated with Spearman's test. Multivariate analysis was performed using logistic regression models. All p values were 2-tailed, and $p < 0.05$ was considered to indicate statistical significance.

Results

Background characteristics of study patients

Table 1 summarizes the characteristics of the study patients. Pathologic examination revealed that all patients had steatosis involving at least 10% of the hepatocytes, and NASH was diagnosed in 43 patients (67.2%). Among 43 patients diagnosed with NASH, 13 patients (30.2%) were diagnosed with stage 3 or 4 fibrosis according to the Brunt classification (Brunt et al. 1999). No significant differences were found between patients with and without NASH with respect to age, sex, body weight,

laboratory data, and degree of steatosis on pathologic evaluation (Supplemental Table 1).

Expression of TIMP1, TIMP2, MMP2, and MMP13 mRNA in liver tissue in patients with NAFLD

Figure 1 compares the gene expression levels of TIMP1, TIMP2, MMP2, and MMP13 based on the quantification of mRNA in the liver tissue of patients with and without NASH. The quantity of MMP2 mRNA was significantly higher in patients with NASH (2.69±1.40, relative expression level) than those without (1.50±0.57; $p < 0.0001$). No significant differences were found in the quantity of TIMP1, TIMP2, and MMP13 mRNA. There were no differences in the quantity of TIMP1, TIMP2, MMP2, and MMP13 mRNA according to the degree of steatosis (data not shown).

Table 1. Characteristics of study patients ($n = 64$).

Age (years)	51.0±15.0
Sex (male/female)	36 (56.3)/28 (43.7)
Body weight (kg)	70.3±11.5
Body mass index (kg/m^2)	27.1±3.5
Alanine aminotransferase (IU/L)	88.5±76.4
Aspartate aminotransferase (IU/L)	54.3±32.5
Gamma-glutamyl transpeptidase (IU)	87.1±64.6
Total bilirubin (mg/dL)	0.71±0.54
Albumin (g/dL)	4.22±0.51
Glucose (mg/dL)*	131.6±61.3
Total cholesterol (mg/dL)*	197.8±39.4
Triglyceride (mg/dL)*	162.1±84.3
Hemoglobin A_1-c (%)	6.07±1.55
Hemoglobin (g/dL)	14.7±1.6
Platelet count (×10^3/μL)	238±70
Ferritin (ng/mL)	231.0±190.7
Steatosis (<30%/30–50%/50–70%/70%≤)**	17 (26.6)/18 (28.1)/19 (29.7)/10 (15.6)
Diagnosis (NASH/simple steatosis)	43 (67.2)/21 (32.8)
Fibrosis (grade 1/2/3/4)**,#	20 (46.5)/10 (23.3)/10 (23.3)/3 (6.9)

NASH, non-alcoholic steatohepatitis.
*Measured under fasting conditions.
**Based on pathologic examination.
#Only in patients with NASH by Brunt classification (Brunt 1999).

Serum levels of TIMP1, MMP2, and hyaluronic acid in patients with NAFLD

Figure 2 compares the levels of TIMP1, MMP2, and hyaluronic acid in serum samples obtained at the time of liver biopsy between patients with and without NASH. Serum levels of TIMP1 and MMP2 showed a significant correlation with liver tissue mRNA levels, respectively, although the correlation was not strong ($p = 0.0003$ and $\rho = 0.472$ for TIMP1, and $p < 0.0001$ and $\rho = 0.534$ for MMP2, Supplemental Figure 1). The serum levels of MMP2 and hyaluronic acid were significantly higher in patients with NASH than in patients without (MMP2, $p = 0.0198$, and hyaluronic acid, $p = 0.0042$). No significant differences were found in the serum levels of TIMP1 between patients with and without NASH.

Univariate and multivariate analyses were performed for factors associated with NASH (Table 2). In the univariate analysis, serum aspartate aminotransferase (AST), MMP2, and hyaluronic acid levels were associated with NASH. In multivariate analysis, serum AST, MMP2, and hyaluronic acid levels were independently associated with NASH.

Expression of MMP2 mRNA in liver tissue and serum levels of MMP2, and hyaluronic acid in NASH patients with mild fibrosis

When excluding patients with NASH and advanced fibrosis (Brunt's fibrosis stage [Brunt et al. 1999] 3 or 4), the quantity of hepatic MMP2 mRNA remained significantly higher in patients with NASH than those without ($p = 0.0010$, Figure 3). Serum levels of MMP2 were also significantly higher in patients with NASH than those without ($p = 0.0020$, Figure 3). No significant differences in serum levels of hyaluronic acid were observed ($p = 0.1296$, Figure 3). In both univariate and multivariate analyses, only serum AST and MMP2 levels were associated with NASH (Table 3).

The predictive value of serum levels of MMP2 and hyaluronic acid were analyzed with receiver-operating characteristic (ROC) analysis. In all patients, serum MMP2 and hyaluronic acid levels had comparable ability for predicting NASH among patients with NAFLD with

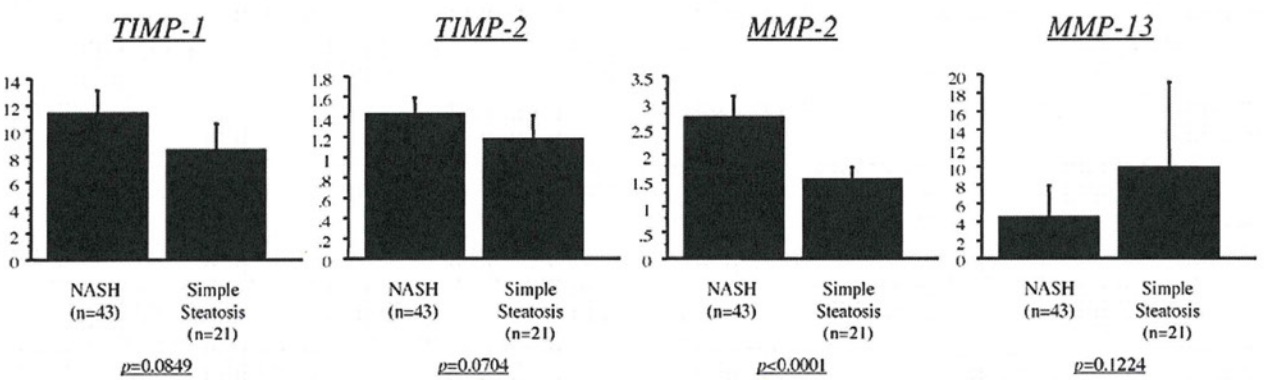

Figure 1. Relative mRNA expression levels of tissue inhibitor metalloproteinase-1 and -2 (TIMP1 and TIMP2), and matrix metalloproteinase 2 and 13 (MMP2 and MMP13) in the liver tissue of patients with nonalcoholic steatohepatitis (NASH) versus simple steatosis.

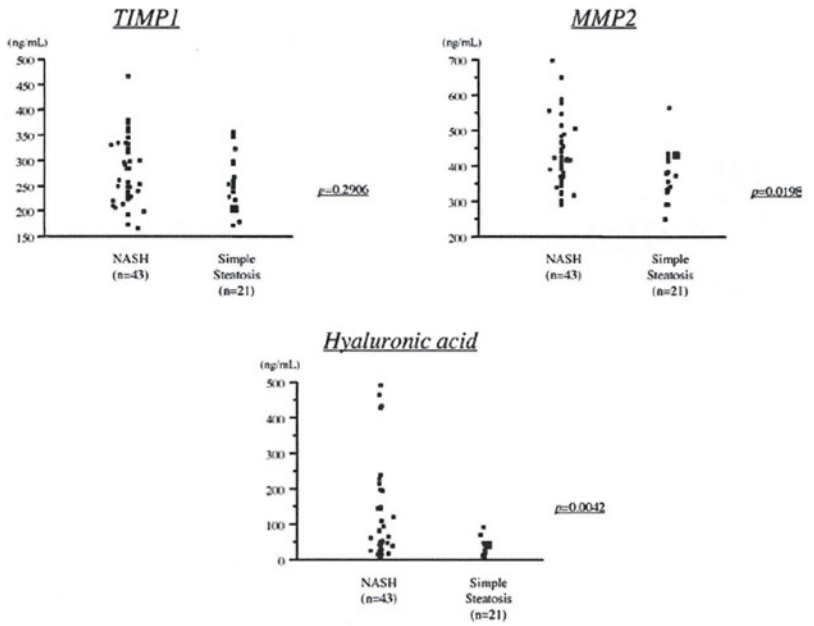

Figure 2. Serum levels of tissue inhibitor metalloproteinase-1 (TIMP1), matrix metalloproteinase-2 (MMP2), and hyaluronic acid in all patients with nonalcoholic steatohepatitis (NASH) versus simple steatosis. TIMP1, 277.4 ± 64.6 ng/mL with NASH vs. 256.5 ± 55.6 ng/mL with simple steatosis; $p = 0.2906$, MMP2, 427.8 ± 95.2 ng/mL with NASH vs. 353.6 ± 55.1 ng/mL with simple steatosis; $p = 0.0198$, and hyaluronic acid, 111.0 ± 131.5 ng/mL with NASH vs. 29.3 ± 21.2 ng/mL with simple steatosis; $p = 0.0042$.

Table 2. Univariate and multivariate analyses for distinguishing between patients with NASH and simple steatosis ($n = 64$).

	Univariate analysis (p value)	Multivariate analysis (p value)	Odds ratio (95% confidence interval)
Age (years)	0.4523	–	
Sex (male/female)	0.9199	–	
Body weight (kg)	0.4524	–	
Body mass index (kg/m^2)	0.2999	–	
Alanine aminotransferase (IU/L)	0.2061	–	
Aspartate aminotransferase (IU/L)	0.0146	0.0258	938.371 (4.9097–922101.2)
Gamma-glutamyl transpeptidase (IU)	0.5724	–	
Total bilirubin (mg/dL)	0.1126	–	
Albumin (g/dL)	0.1959	–	
Glucose (mg/dL)*	0.1898	–	
Total cholesterol (mg/dL)*	0.2338	–	
Triglyceride (mg/dL)*	0.1696	–	
Hemoglobin A_1-c (%)	0.9370	–	
Hemoglobin (g/dL)	0.5974	–	
Platelet count (×10^3/μL)	0.0613	–	
Ferritin (ng/mL)	0.5443	–	
TIMP1 (ng/mL)	0.2224	–	
MMP2 (ng/mL)	0.0058	0.0275	364.171 (3.9968–174225.9)
Hyaluronic acid (ng/mL)	0.0228	0.0351	23346.68 (32.5694–298598)
Steatosis (<30%/30–50%/50–70%/70%≤)**	0.8713	–	

NASH, non-alcoholic steatohepatitis; TIMP1, tissue inhibitor metalloproteinase-1; MMP2, matrix metalloproteinase-2.
*Measured during fasting conditions.
**Based on pathologic examination.

similar area under the ROC curves (AUROC) (MMP2, 0.73 and hyaluronic acid, 0.77, Supplemental Figure 2). When NASH patients with advanced fibrosis were excluded, the ability of serum hyaluronic acid levels to predict NASH decreased (AUROC, 0.63), whereas the predictive ability of serum MMP2 levels remained similar (AUROC, 0.74, Supplemental Figure 3).

Discussion

In the present study, we observed enhanced gene expression of MMP2 in liver tissue, along with elevated serum levels of MMP2, both of which showed the correlation, in patients with NASH compared to those with simple steatosis. MMP2 expression reportedly increases during the

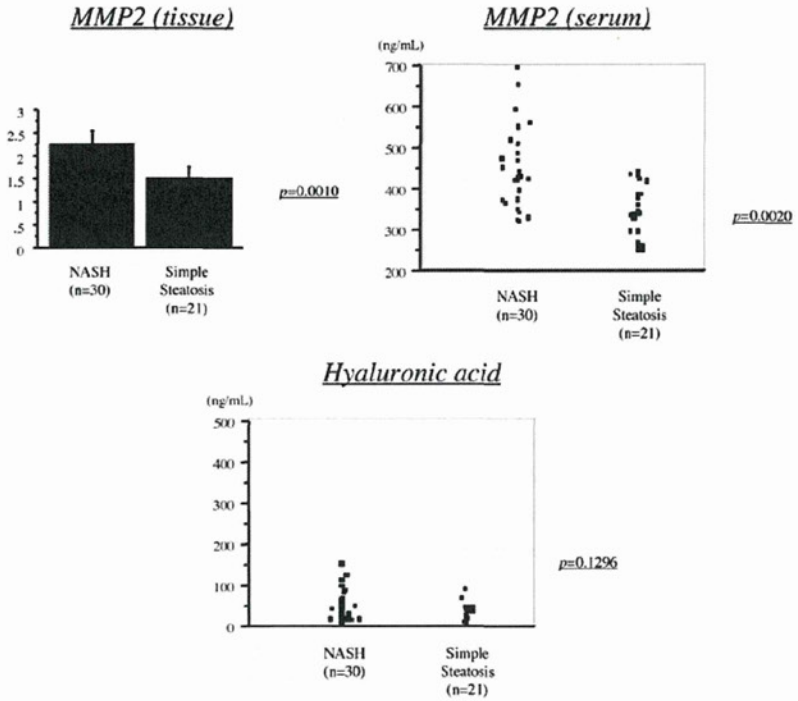

Figure 3. Quantity of matrix metalloproteinase-2 (MMP2) mRNA in liver tissue and serum levels of MMP2, and hyaluronic acid in nonalcoholic steatohepatitis (NASH) patients without advanced fibrosis versus patients with simple steatosis. MMP2 mRNA, 2.23 ± 0.84 with NASH vs. 1.50 ± 0.57 with simple steatosis; p = 0.0010, serum levels of MMP2, 441.8 ± 99.6 ng/mL with NASH vs. 353.6 ± 55.1 ng/mL with simple steatosis; p = 0.0020, and serum levels of hyaluronic acid, 143.1 ± 31.1 ng/mL with NASH vs. 130.3 ± 63.1 ng/mL with simple steatosis; p = 0.1296.

Table 3. Univariate and multivariate analyses for distinguishing patients with NASH and simple steatosis, excluding NASH patients with advanced fibrosis (n = 51).

	Univariate analysis (p value)	Multivariate analysis (p value)	Odds ratio (95% confidence interval)
Age (years)	0.7699	–	
Sex (male/female)	0.9730	–	
Body weight (kg)	0.3069	–	
Body mass index (kg/m^2)	0.2221	–	
Alanine aminotransferase (IU/L)	0.1769	–	
Aspartate aminotransferase (IU/L)	0.0309	0.0251	240.057 (3.5678–72252.5)
Gamma-glutamyl transpeptidase (IU)	0.7185	–	
Total bilirubin (mg/dL)	0.1344	–	
Albumin (g/dL)	0.3718	–	
Glucose (mg/dL)*	0.5584	–	
Total cholesterol (mg/dL)*	0.5173	–	
Triglyceride (mg/dL)*	0.1327	–	
Hemoglobin A_1-c (%)	0.7368	–	
Hemoglobin (g/dL)	0.8608	–	
Platelet count (×10^3/μL)	0.5635	–	
Ferritin (ng/mL)	0.8109	–	
TIMP1 (ng/mL)	0.2302	–	
MMP2 (ng/mL)	0.0047	0.0068	2759.72 (19.7697–2163013)
Hyaluronic acid (ng/mL)	0.1007	–	
Steatosis (<30%/30–50%/50–70%/70%≤)**	0.2877	–	

NASH, non-alcoholic steatohepatitis; TIMP1, tissue inhibitor metalloproteinase-1; MMP2, matrix metalloproteinase-2.
*Measured during fasting conditions.
**Based on pathologic examination.

progression of liver fibrosis (Ebata et al. 1997; Hemmann et al. 2007), and our results indicated that liver fibrosis is proceeding in patients with NASH.

NASH is usually diagnosed by histological evaluation of specimens obtained by liver biopsy and this is currently the only reliable and accepted method for the evaluation of liver fibrosis. However, liver biopsy is invasive and carries the risk of intraperitoneal bleeding. Therefore, noninvasive indicators of NASH in NAFLD patients would be important. Several biomarkers have been studied as indicators of NASH in patients with NAFLD (Malik et al. 2009; Miele et al. 2009). The serum level of hyaluronic acid is an important marker for the identification of patients with NASH. Because serum hyaluronic acid levels increase with the progression of liver fibrosis (Adams 2011) and the increase can simply reflect accumulated fibrosis in the liver as a result of the progression of NASH, it may not be an indicator of NASH but with mild fibrosis (i.e. early stage of NASH). Although serum hyaluronic acid levels were significantly higher in patients with NASH than those without NASH in the present study, we failed to find significant differences in serum hyaluronic acid levels between NASH patients with mild fibrosis and those without NASH. Whereas the AUROC for serum hyaluronic acid level in predicting NASH was more than 0.7 in patients including advanced fibrosis in the study by Malik et al. and in the present study, it decreased from 0.77 to 0.63 when focusing on patients with mild fibrosis in the present study. Serum hyaluronic acid levels, therefore, do not appear to be useful for distinguishing NASH patients with mild fibrosis from patients without NASH. In contrast, the AUROC for serum MMP2 levels in predicting NASH remains greater than 0.73 even in the subpopulation with mild fibrosis. In clinical practice, it will be important to identify NASH patients with mild fibrosis, before the progression of liver fibrosis caused by NASH, from NAFLD patients. Serum MMP2 levels may be useful for this purpose.

Conclusion

In patients with NASH, gene expression of MMP2, a protein associated with liver fibrosis, was enhanced in the liver tissue and serum levels of MMP2 were increased, indicating the initiation of liver fibrosis in this subpopulation. These results were also observed when NASH patients with advanced fibrosis were excluded. MMP2 may be a noninvasive indicator of early stage of NASH in patients with NAFLD.

Declaration of interest

The authors declare no conflicts of interest.

References

Adams LA. (2011). Biomarkers of liver fibrosis. *J Gastroenterol Hepatol* 26:802–809.

Angulo P. (2002). Nonalcoholic fatty liver disease. *N Engl J Med* 346:1221–1231.

Brunt EM, Janney CG, Di Bisceglie AM, Neuschwander-Tetri BA, Bacon BR. (1999). Nonalcoholic steatohepatitis: A proposal for grading and staging the histological lesions. *Am J Gastroenterol* 94:2467–2474.

Chitturi S, Farrell GC, Hashimoto E, Saibara T, Lau GK, Sollano JD; Asia-Pacific Working Party on NAFLD. (2007). Non-alcoholic fatty liver disease in the Asia-Pacific region: Definitions and overview of proposed guidelines. *J Gastroenterol Hepatol* 22:778–787.

Clark JM, Brancati FL, Diehl AM. (2003). The prevalence and etiology of elevated aminotransferase levels in the United States. *Am J Gastroenterol* 98:960–967.

Ebata M, Fukuda Y, Nakano I, Katano Y, Fujimoto N, Hayakawa T. (1997). Serum levels of tissue inhibitor of metalloproteinases-2 and of precursor form of matrix metalloproteinase-2 in patients with liver disease. *Liver* 17:293–299.

Fassio E, Alvarez E, Domínguez N, Landeira G, Longo C. (2004). Natural history of nonalcoholic steatohepatitis: A longitudinal study of repeat liver biopsies. *Hepatology* 40:820–826.

Hamaguchi M, Kojima T, Itoh Y, Harano Y, Fujii K, Nakajima T, Kato T, Takeda N, Okuda J, Ida K, Kawahito Y, Yoshikawa T, Okanoue T. (2007). The severity of ultrasonographic findings in nonalcoholic fatty liver disease reflects the metabolic syndrome and visceral fat accumulation. *Am J Gastroenterol* 102:2708–2715.

Hashimoto E, Yatsuji S, Kaneda H, Yoshioka Y, Taniai M, Tokushige K, Shiratori K. (2005). The characteristics and natural history of Japanese patients with nonalcoholic fatty liver disease. *Hepatol Res* 33:72–76.

Hemmann S, Graf J, Roderfeld M, Roeb E. (2007). Expression of MMPs and TIMPs in liver fibrosis - a systematic review with special emphasis on anti-fibrotic strategies. *J Hepatol* 46:955–975.

Kojima S, Watanabe N, Numata M, Ogawa T, Matsuzaki S. (2003). Increase in the prevalence of fatty liver in Japan over the past 12 years: Analysis of clinical background. *J Gastroenterol* 38:954–961.

Malik R, Chang M, Bhaskar K, Nasser I, Curry M, Schuppan D, Byrnes V, Afdhal N. (2009). The clinical utility of biomarkers and the nonalcoholic steatohepatitis CRN liver biopsy scoring system in patients with nonalcoholic fatty liver disease. *J Gastroenterol Hepatol* 24:564–568.

Matteoni CA, Younossi ZM, Gramlich T, Boparai N, Liu YC, McCullough AJ. (1999). Nonalcoholic fatty liver disease: A spectrum of clinical and pathological severity. *Gastroenterology* 116:1413–1419.

Miele L, Forgione A, La Torre G, Vero V, Cefalo C, Racco S, Vellone VG, Vecchio FM, Gasbarrini G, Rapaccini GL, Neuman MG, Grieco A. (2009). Serum levels of hyaluronic acid and tissue metalloproteinase inhibitor-1 combined with age predict the presence of nonalcoholic steatohepatitis in a pilot cohort of subjects with nonalcoholic fatty liver disease. *Transl Res* 154:194–201.

Musso G, Gambino R, Cassader M. (2010). Non-alcoholic fatty liver disease from pathogenesis to management: An update. *Obes Rev* 11:430–445.

Torres DM, Harrison SA. (2008). Diagnosis and therapy of nonalcoholic steatohepatitis. *Gastroenterology* 134:1682–1698.

EXPERIMENTAL CELL RESEARCH 319 (2013) 113–121

Available online at www.sciencedirect.com

SciVerse ScienceDirect

journal homepage: www.elsevier.com/locate/yexcr

Research Article

Leucine-rich repeat-containing G protein-coupled receptor 5 regulates epithelial cell phenotype and survival of hepatocellular carcinoma cells

Mariko Fukuma[a], *Keiji Tanese*[b], *Kathryn Effendi*[a], *Ken Yamazaki*[a], *Yohei Masugi*[a], *Mariko Suda*[a], *Michiie Sakamoto*[a,*]

[a]*Department of pathology, Keio University School of Medicine, Shinjuku-ku, Tokyo 160-8582, Japan*
[b]*Department of dermatology, Keio University School of Medicine, Shinjuku-ku, Tokyo 160–8582, Japan*

ARTICLE INFORMATION

Article Chronology:
Received 28 June 2012
Received in revised form
11 October 2012
Accepted 26 October 2012
Available online 2 November 2012

Keywords:
LGR5
GPR49
Hepatocellular carcinoma
Morphology
Motility

ABSTRACT

The leucine-rich repeat containing G protein-coupled receptor 5 (LGR5), also known as GPR49, is a seven-transmembrane receptor that is expressed in stem cells of the intestinal crypts and hair follicles of mice. LGR5 is overexpressed in some types of human cancer, and is one of the target genes of the Wnt signaling pathway. To explore the function of LGR5 in cancer cells, stable hepatocellular carcinoma (HCC) cell lines expressing FLAG-tagged LGR5 were established. Overexpression of LGR5 resulted in changes in cell shape from an extended flat (mesenchymal) phenotype to a round aggregated (stem cell-like) phenotype. Cells transfected with LGR5 showed higher colony forming activity, and were more resistant to a cytotoxic drug than cells transfected with empty vector. Overexpression of LGR5 inhibited cell motility. LGR5-transfected cells formed nodule type tumors in the livers of immunodeficient mice, whereas empty vector-transfected cells formed more invasive tumors. Down-regulation of LGR5 changed the morphology of HCC cells from the aggregated phenotype to an extended spindle phenotype, and cell motility was increased. This is the first study reporting the functional role of LGR5 in the biology of HCC cells, and the results suggest that aberrant expression of LGR5 regulates epithelial cell phenotype and survival.

Introduction

The leucine-rich repeat-containing G protein-coupled receptor 5 (LGR5), aliases G protein-coupled receptor 49 (GPR49), FEX, GPR67, GRP49, HG38, MGC117008, is structurally related to members of the glycoprotein hormone receptor family. In mice, deficiency of this gene causes neonatal lethality as a result of ankyloglossia [1]. LGR5 deficiency also induces premature differentiation of Paneth cells [2]. Recent studies from the Netherlands showed that in a mouse model, the homolog of this gene was a marker of intestinal and hair follicle stem cells. Introduction of an adenomatous polyposis coli (APC) mutation into LGR5-expressing cells increased the incidence of adenomas in mouse intestinal epithelial cells [3–5].

*Correspondence to: Department of pathology, Keio University School of Medicine, 35 Shinanomachi, Shinjuku-ku, Tokyo 160-8582, Japan. Fax: +81 3 3353 3290.
E-mail address: msakamot@z5.keio.jp (M. Sakamoto).

0014-4827/$ - see front matter © 2012 Elsevier Inc. All rights reserved.
http://dx.doi.org/10.1016/j.yexcr.2012.10.011

LGR5 has been reported to be upregulated in several tumors. We have previously shown that expression of LGR5 in the noncancerous liver was very low, however LGR5 is frequently overexpressed in hepatocellular carcinoma (HCC) with β-catenin mutations [6]. Although mutations of β-catenin are found in nearly 40% of HCC, the LGR5 has not been reported as the marker of hepatocyte, nor mentioned as a marker gene for liver regeneration. LGR5 also has been identified as a gene responsible to promote cell proliferation and tumor formation in basal cell carcinoma (BCC), a common malignant tumor of the skin [7]. High levels of LGR5 expression were also reported in colon and ovarian carcinomas [8], and we have shown that a high level of LGR5 expression in colorectal cancer was significantly correlated with tumor stage [9]. One study using colorectal cancer cell lines showed that suppression of LGR5 expression enhances tumorigenesis and is linked to a more mesenchymal phenotype [10].

There are some evidences suggest that LGR5 is a downstream target gene of Wnt signaling pathway [2,6,11,12]. The Wnt signaling pathway comprises a vast number of protein interactions and plays a critical role in morphogenesis and tumorigenesis. To date, three main pathways related to Wnt signaling have been identified: the β-catenin-dependent, planar cell polarity, and Wnt/Ca^{2+} pathways [13]. The β-catenin-dependent pathway, otherwise known as the canonical pathway, has been the most intensively studied. Mutations or deletions in AXN1/2 or APC genes inhibit the phosphorylating activity of GSK-3β, thereby stabilizing cytoplasmic β-catenin, and provoking aberrant cellular gene expression. Mutations at sites that affect β-catenin phosphorylation also cause cytoplasmic accumulation of β-catenin and lead to dysregulation of the pathway. Recently, LGR5 was reported to be a receptor of R-spondins which were known to be a potent family protein mediating Wnt/β-catenin and Wnt/PCP signaling [11,12,14]. Acquirement of stem cell-like properties in various tumors have greatly increased the possible role of these cells in tumorigenesis [15,16]. Upregulation of LGR5 in several tumors with increased Wnt signaling pathway suggests the possible role of LGR5 gene in oncogenesis and morphogenesis [6–9]. However, the functional role of LGR5 in tumor cells is still poorly understood. In this study, we aimed to analyze the function of LGR5 in hepatocellular carcinoma cells.

Materials and methods

Cell culture and chemicals

Cells were cultured in RPMI 1640 supplemented with 10% fetal bovine serum, 100 U/ml of penicillin and 100 μg/ml of streptomycin [6,9]. HepG2 containing a deletion of exon 3 of the β-catenin gene and PLC/PRF/5 containing a deletion of exon 4 of the AXIN1 were used as cell lines with activated Wnt signaling and high levels of LGR5 mRNA[17]. KYN2 cells were used as a cell line with low expression of LGR5 mRNA [6,9].

Plasmids, transfection, and establishment of stable transfectants

A FLAG-tagged LGR5 expression vector (LGR5-FL) was constructed by inserting the full-length coding cDNA for human LGR5 (RZPD, Berlin, Germany) into the Bgl II site of p3XFLAG-CMV-14 (Sigma-Aldrich, St. Louis, MO, USA). KYN-2 cells were transfected with LGR5-FL or empty vector using Lipofectamine LTX reagent (Invitrogen, Carlsbad, CA, USA). Production of LGR5-FL protein was detected by confocal laser scanning microscopy (LSM510, Carl Zeiss, Germany) and western blot analysis, using the FLAG M2 antibody (Sigma-Aldrich). F-actin was stained with TexasRed X-phalloidin (Molecular Probes, Eugene, OR, USA) and nucleus was stained with VECTASHIELD Mounting Medium with DAPI (Vector Laboratories Inc. Burlingame, CA, USA). Anti-E-cadherin (ALX-804-201-C100, Enzo Life Sciences, Inc.) and anti-β-catenin (E-5, Santa Cruz Biotechnology, Inc.) antibodies were used for immunofluorescent staining. Colonies that formed in 0.3% soft agar medium containing G418 (Invitrogen) were picked and propagated. Each colony was purified by three sequential series of limiting dilutions. Ultimately, six LGR5-transfected clones (KY-B1, KY-G1, KY-G2, KY-G6, KY-F3, and KY-S1) and five empty vector-transfected clones (KY-V2, KY-V3, KY-V4, KY-V5, and KY-V6) were established. Protein levels were analyzed by western blotting and mRNA levels were analyzed by quantitative PCR. Canonical Wnt signaling activity was measured with the TCF-luciferase reporter system (TOPflash/FOPflash, Upstate Millipore Co.), and the results are shown as the ratio of TOPflash to FOPflash (TOP/FOP).

Quantitative polymerase chain reaction (qPCR)

Total RNA was isolated from cells using the RNeasy Mini Kit, including DNase treatment (Qiagen KK, Tokyo, Japan). cDNA was synthesized using the PrimeScript® RT reagent kit (Perfect Real Time; Takara Bio, Shiga, Japan), and qPCR was performed on a Thermal Cycler Dice Real Time System using SYBR *Premix Ex Taq*™ (Perfect Real Time; Takara Bio). The primer sequences for qPCR were as follows: GAPDH forward, 5′–ATCATCCCTGCCTCTACTGG-3′; GAPDH reverse, 5′–TTTCTAGACGGCAGGTCAGGT-3′; LGR5 forward, 5′–GAGGATCTGGTGAGCCTGAGAA-3′; LGR5 reverse, 5′–CATAAGTGATGCTGGAGCTGGTAA-3′; RSPO1 forward, 5′–AAGGCTGTGAGCTCTGCTCT-3′; RSPO1 reverse, 5′–ATGTCGTTCCTCTCCAGCAG3′. GAPDH was used as a reference. Fold induction values were calculated using the $2^{-\Delta\Delta\ Ct}$ method. All experiments were performed in triplicate and repeated at least three times in separate experiments; representative data are shown.

Cell proliferation, cell migration, and cytotoxicity assays

Cells were plated in 24-well dishes, and the number of cells was counted in a hemocytometer after staining with trypan blue. Ratio number of cells represents the total mean number of LGR5-overexpressing cells or empty vector cells for each day compared to the total mean number of cells at day 0. RNA interference experiments were performed using siRNA. The target sequences were as follows: LGR5-585, 5′–GAA CAA AAU ACA CCA CAUA-3′; LGR5-662, 5′–GAA UCC ACU CCC UGG GAAA-3′. AllStars Negative Control siRNA (Qiagen) was used as a control. Cells were transfected with the final concentration of 10 nM siRNA using Lipofectamine RNAiMAX transfection reagent (Invitrogen).

For cytotoxicity tests, cells were treated with puromycin for 20 h, washed with PBS and covered with growth medium containing 0.3% agar. Cells were cultured for 2 weeks with occasional replenishment of the medium. Colonies were stained

with nitro blue tetrazolium reagent and photographed for counting. For cell migration assays, cells were placed in six-well dishes and incubated for two days. The confluent monolayer cultures were scratched and photographed after 24 h. The width of each scratch was measured at ten points and more than five scratches were measured for each group. For RNA interference assays, cells were transfected with siRNAs for 20 h and replated in six-well dishes. The monolayer cultures that formed 24 h later were scratched and photographed as described previously.

Tumor formation assays

Clones containing LGR5-FL or empty vector were transplanted into the subcapsular region of the livers of NOG mice (NOD/Shi-scid/IL-2γ−/−) at 5×10^6 cells per mouse. The tumors that formed in the liver were resected, fixed with 10% neutral-formalin, and used for histological analysis. For metastasis assays, cells were inoculated into the subcapsular region of the spleens of NOG mice, and tumors that formed in the liver were used for histological analysis.

Statistical analysis

Differences were assessed for statistical significance using Student's *t*-test, with the level of significance being $P<0.05$.

Results

Establishment of LGR5-overexpressing clones

To determine the function of LGR5 in cancer cells, stable clones containing the LGR5 gene were established. We have tested several commercially available anti-LGR5 antibodies, however, we could not obtain good results in order to detect LGR5 protein expression in HCC tissue. Thus, we constructed a FLAG-tagged LGR5-expression vector (LGR5-FL), and production of the protein was detected by immunofluorescence microscopy and western blot analysis using anti-FLAG antibody. When LGR5-FL was transfected into KYN-2 cells, the protein was localized mostly in the cytoplasm and cytoplasmic membrane (Fig. 1A). To establish stable clones, LGR5-FL or empty vector was transfected into KYN-2 cells, and G418-resistant colonies that formed in soft agar medium were purified by three series of limiting-dilution propagations. Six clones stably transfected with LGR5-FL (KY-B1, KY-G1, KY-G2, KY-G6, KY-F3, KY-S1) and five clones stably transfected with empty vector (KY-V2, KY-V3, KY-V4, KY-V5, KY-V6) were isolated. The LGR5 protein (~100 kD) was detected by western bot analysis (Fig. 1B), and mRNA levels were measured by qPCR (Fig. 1C). The KY-G1 and KY-S1 transfectants expressed high levels of LGR5 protein and mRNA. The protein and mRNA levels in each of the clones were well correlated, and the same levels were maintained after several passages. Only the results for three vector-transfectants are shown in Fig. 1B and C, but the other clones showed similar results.

Phase contrast microscopy showed that LGR5-overexpressing KY-G1 and KY-S1 cells had a round shape and aggregated together, whereas KY-V2 and KY-V3 cells had a flat extended shape and spread on the culture dishes (Fig. 1D). LGR5-transfectants stacked up on the surface of the culture dishes, whereas empty vector–transfectants formed flat monolayers (Fig. 1E). Phalloidin staining showed strong F-actin signals between KY-G1 cells (so-called cortical actin), whereas KY-V2 cells showed a flat extended shape with F-actin in the cytoplasm (Fig. 1F). Distinct fluorescent signals of E-cadherin were located between KY-G1 cells (Fig. 1G). Similar distribution of β-catenin was also seen in KY-G1 and KY-V2 cells, respectively (Fig. 1H). Accumulation of β-catenin in nuclei which is often seen in cell with activated Wnt signaling could not be detected in LGR-5 overexpressing KY-G1 cells. Non-adherent cultures of KY-G1 cells formed spherical shapes and most of the cells in the center survived intact, whereas KY-V2 cells formed irregular spheres and some of these had a necrotic area at the center (Fig. 1G).

Overexpression of LGR5 promotes HCC cell viability, enhances colony formation, and decreases cell motility

The rates of proliferation of KY-G1 and KY-V2 cells were identical until cell numbers reached a maximum, however, KY-G1 cells survived longer in overgrowth conditions (Fig. 2A). Substantial numbers of KY-G1 cells survived after two weeks in overgrowth culture, whereas KY-V2 cells detached from the surface of the dishes and only a small proportion of cells survived in over-growth culture (Fig. 2B). In addition, KY-G1 cells were more resistant to the toxicity of puromycin (Fig. 2C), and also formed soft agar colonies more efficiently than KY-V2 cells (Fig. 2D). The motility of the cells was measured by performing scratch tests on confluent cell cultures. Retardation of cell migration was observed as early as 5 h in KY-G1 cells (data not shown), and scratch scars were repaired more rapidly at 24 h in KY-V2 cell cultures than in KY-G1 cell cultures (Fig. 2E). The reduction ability of LGR5-overexpressing cells to migrate after scratch wound assay was also previously reported in colorectal carcinoma cell lines [10].

LGR5-overexpressing HCC cells forms nodular tumors with decreased infiltration and metastatic foci

To further evaluate the function of LGR5 in vivo, KY-G1 or KY-V2 cells were transplanted into the subcapsular region of the livers of NOG mice. KY-G1 cells formed tumors with trabecular pattern in the liver, while KY-V2 cells formed tumors with ill trabecular pattern (Fig. 3A a, b). Expression of LGR5-FL was detected in the tumors formed by KY-G1 cells but not in the tumors formed by KY-V2 cells (Fig. 3A a, b inserts). Reticulum staining showed a trabecular pattern in the KY-G1 tumors, whereas a solid pattern was observed in the KY-V2 tumors (Fig. 3A c, d). Infiltration into the vicinal muscle tissues was rare in the tumors formed by KY-G1 cells, but occasionally seen in the tumors formed by KY-V2 cells (Fig. 3A e, f). When KY-G1 cells were transplanted into the subcapsular region of the spleen, the number of metastatic foci in the liver, and the number of micrometastases into the portal veins was lower, compared with transplantation of KY-V2 cells (Fig. 3B a–c). In addition, tumors formed by KY-V2 cells showed a wider area of hemorrhagic necrosis compared with those formed by KY-G1 cells.

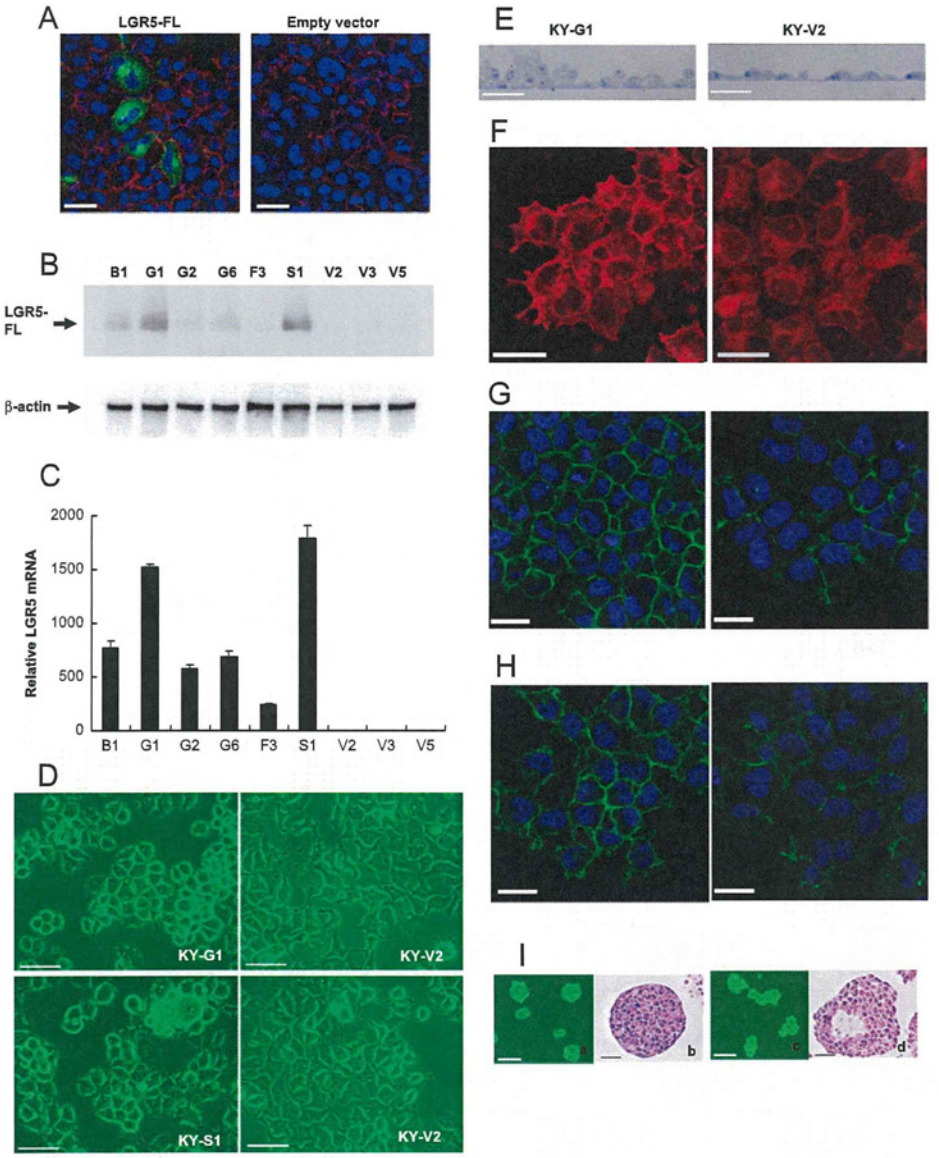

Fig. 1 – Establishment of LGR5-overexpressing clones. A: Immunofluorescent staining of KYN-2 cells transiently transfected with LGR5-FL or empty vector. Cells were stained with anti-FLAG antibody. Green: LGR5. Red: F-actin. Blue: nuclei. Bar, 50 μm. B: Western blot analysis of LGR5-overexpressing clones (KY-B1, KY-G1, KY-G2, KY-G6, KY-F3, KY-S1). KY-V2, KY-V3 and KY-V5 were stable transfectants containing empty vector. Blots were stained with anti-FLAG antibody (upper) or anti-β-actin antibody (lower). C: Expression of LGR5 mRNA in stable transfectants. Relative LGR5 mRNA level was shown as fold increase when the average level of non-transfected KYN-2 was set at 1. D: Morphology of clones containing LGR5-FL (KY-G1 and KY-S1) or empty vector (KY-V2 and KY-V3). (Bar, 100 μm) E: Vertical sections of 3-day cultures. KY-G1 and KY-V2 cells were embedded in EPON resin and sliced sections were stained with toluidine blue. F: Distribution of F-actin. F-actin was visualized by staining with phalloidin. Bar, 100 μm. G: Localization of E-cadherin (Green: E-cadherin, Blue: nuclei, Bar, 50 μm). H: Localization of β-catenin (Green: E-cadherin, Blue: nuclei, Bar, 50 μm). I: Morphology of non-adherent cultures of KY-G1 (a, b) and KY-V2 (c, d). Photographs show phase contrast microscopy (a, c. Bar, 200 μm) and HE staining of paraffin embedded sections (b, d. Bar, 500 μm). E-I: KY-G1 (left column), KY-V2 (right column). (For interpretation of the references to color in this figure, the reader is referred to the web version of this article.)

Down-regulation of LGR5 in HCC cells transforms cells to a loosely associated morphology and increased cell motility

To determine whether the characteristics of the KY-G1 cells were indeed due to the expression of higher levels of LGR5, we examined the effect of down-regulating LGR5 using siRNA. HepG2 cells were transfected with two siRNA sequences (si585 and si662) and LGR5 mRNA levels were analyzed by qPCR. LGR5 mRNA levels were significantly decreased 24–96 h after transfection of siRNAs against LGR5 (Supplementary Fig. 1; only 48 h data is shown). si662 suppressed expression of LGR5 more efficiently than si585, and similar results were obtained with

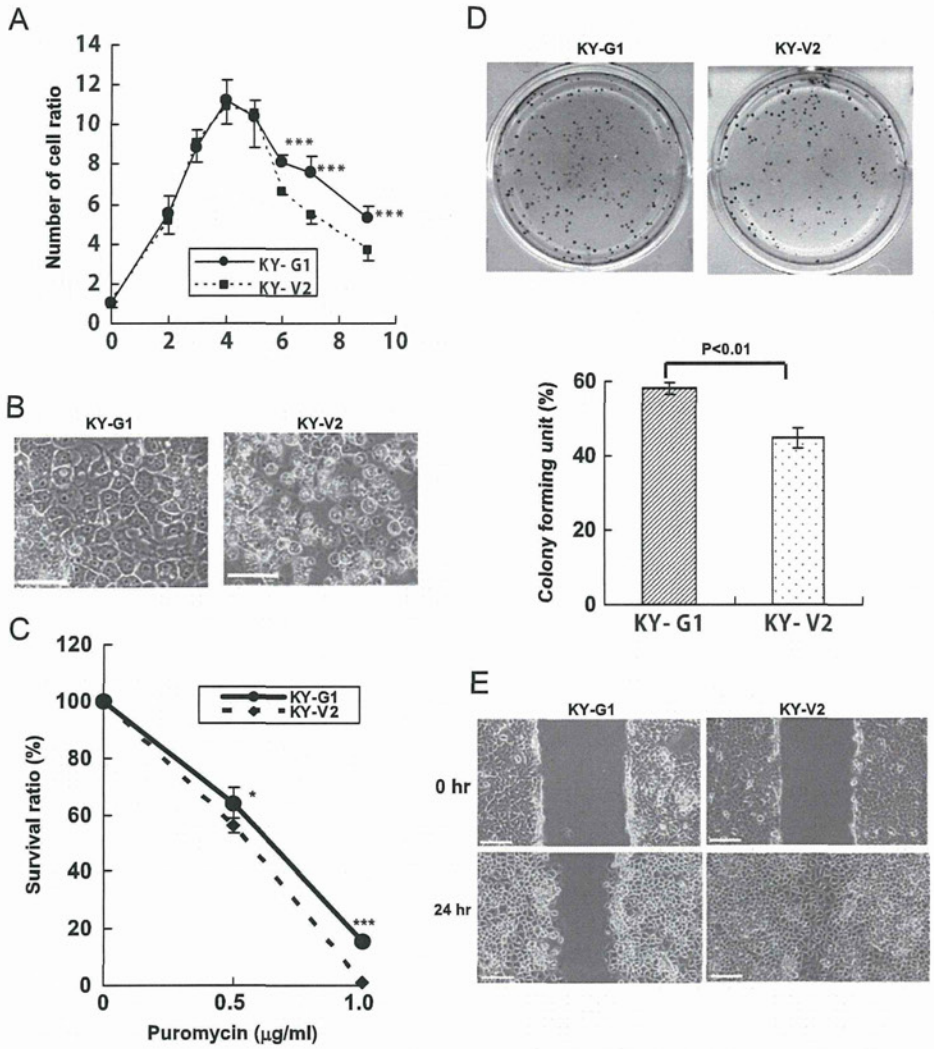

Fig. 2 – Characterization of LGR5-overexpressing clones. A: Growth and survival of KY-G1 and KY-V2 cells. High levels of LGR5 expression did not affect the growth rate of the cells; however, KY-G1 cells survived longer in overgrowth conditions. ***: $P<0.01$. B: Morphology of clones after 2 weeks of culture. (Bar, 100 μm) Viable cells were still observed in the KY-G1 culture, but few cells were alive in the KY-V2 culture. C: Resistance to cytotoxicity. Cells were treated with puromycin for 20 h, and cultured under soft agar medium. Cells with high expression of LGR5 were more resistant to the cytotoxic effect of puromycin. *: $P<0.05$. ***: $P<0.01$. D: Colony formation. Upper: 500 cells were cultured in soft agar plates for 2 weeks. Lower: quantitative assay of colony forming activity. Colony forming unit: ratio of colonies formed to number of cells inoculated (%). High levels of LGR5 expression enhanced colony formation. E: Motility assay. Confluent cell layers were scratched and photographed at 0 and 24 h. High levels of LGR5 expression inhibited cell motility. (Bar, 200 μm).

PLC/PRF/5 cells (Supplementary Fig. 2). When LGR5 mRNA was down-regulated with siRNA, the tight aggregated morphology of HepG2 cells was transformed to a loosely associated morphology. Some of the cells began to migrate away from the cell aggregates (Fig. 4A, upper column). The strongly staining cortical actins between the cells became extended filaments when expression of LGR5 was down-regulated (Fig. 4B, upper column). siRNA directed against LGR5 showed similar effects in PLC/PRF/5 cells (Fig. 4A and B, lower columns). The cortical actin between the cells became long, extended filaments. Down-regulation of LGR5 also increased cell motility. When HepG2 cells were treated with si585 or si662, scratched scars were repaired more rapidly than in cells treated with siControl (Fig. 5A, C). Similar results were obtained when PLC/PRF/5 cells were treated with siRNA directed against LGR5 (Fig. 5B, C).

Discussion

To determine the function of LGR5 in tumor cells, we carefully investigated cell clones containing a FLAG-tagged expression vector (LGR5-FL). The LGR-5 transfected clone (KY-G1) became rounded and formed aggregates when grown as an adherent culture. It formed spherical bodies when propagated in suspension culture, more resistance to cytocidal conditions, and showed decreased migratory activity. The Wnt signaling pathway is an

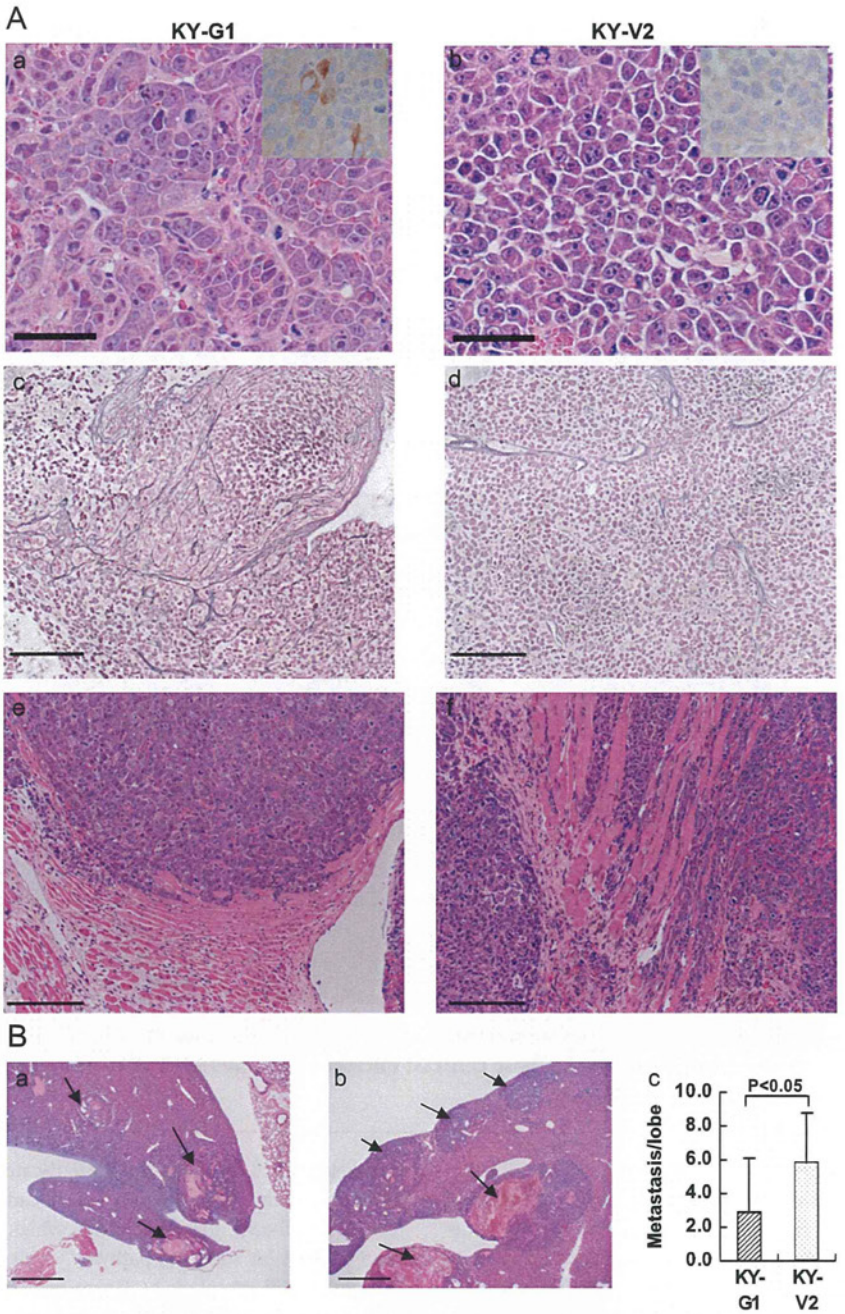

Fig. 3 – Histological analysis of tumors formed by KY-G1 or KY-V2 clones in the livers of NOG mice. A: KY-G1 (left) and KY-V2 (right) cells were transplanted into the subcapsular region of the livers of mice. Tumors were resected and thin sections were stained with HE (a, b. Bar, 100 μm)(e, f. Bar, 200 μm) or silver impregnation (c, d. Bar, 200 μm). Inserts show immunohistochemical staining with anti-FLAG antibody (a, b). B: KY-G1 (a) and KY-V2 (b) cells were transplanted into subcapsular region of the spleens of NOG mice. Tumors that formed in the livers were fixed and stained with HE (Bar 500 μm). Arrows show metastatic foci in the liver. The number of metastases was quantified (c). Tumors larger than 0.25 mm in diameter were counted. High levels of LGR5 expression inhibited metastasis to the liver.

important pathway for morphogenesis and maintaining the stemness of cells. Sphere formation, colony formation and resistance to cytotoxic drugs are important criteria for the stemness of cells. LGR5-overexpressing KY-G1 cells formed tightly packed spheres, with viable cells extending from the surface to the center when cultured under non-adherent conditions, whereas KY-V2 cells containing the empty vector formed loose, irregular spheres, and some cells in the central area showed signs of necrosis. KY-G1 cells were also more resistant to a cytocidal environment, survived longer under nutrient depletion conditions, and were more resistant to the cytocidal effect of puromycin. The differences between LGR5-transfected and vector-transfected cells were rather marginal, which may be affected by the

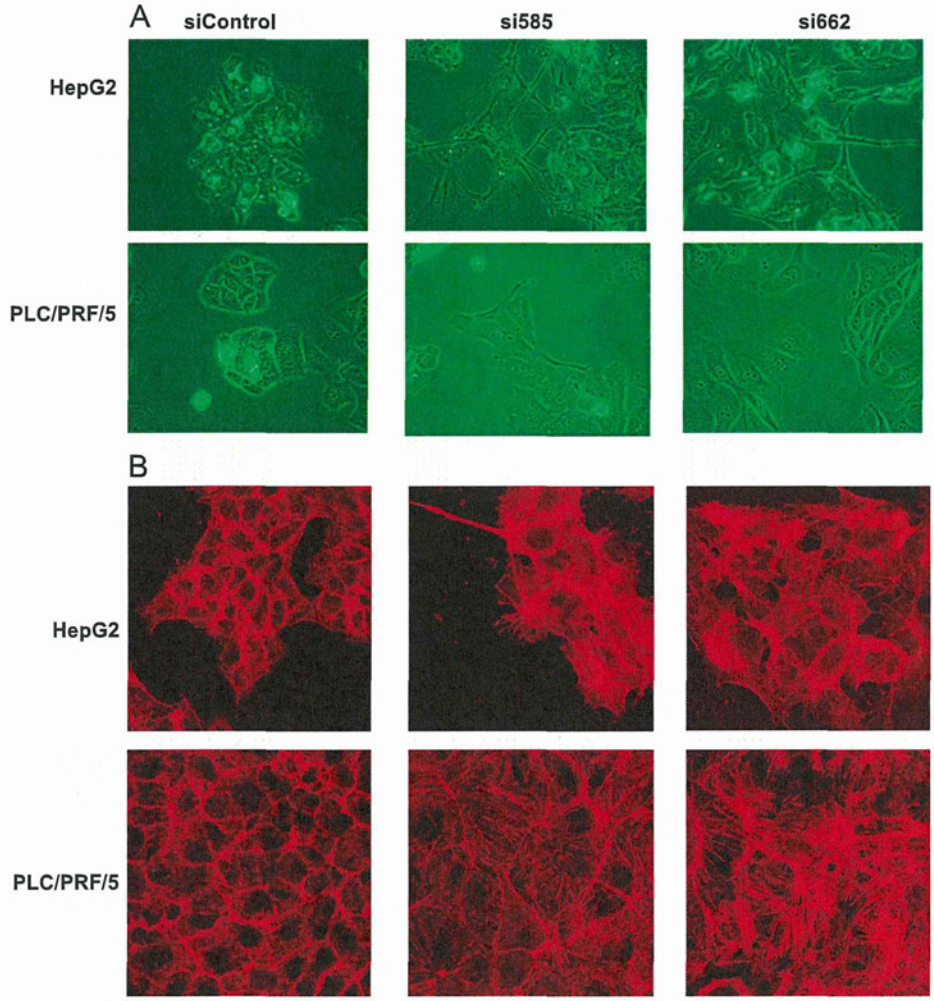

Fig. 4 – Down-regulation of LGR5 in HCC cell lines by treatment with siRNAs. HepG2 and PLC/PRF/5 cells were transfected with siControl, si585 or si662, and cultured for 2 days. A: Phase contrast microscopy. (× 400) B: Immunofluorescent microscopy. Actin filaments were stained with phalloidin. (× 400).

presence of substantial expression of LGR4 in parental KYN-2 cells. LGR4, LGR5, and LGR6 have homology with about 50% identity between each other at the amino acid level, and may compensate each other functions [18]. Since LGR4 is constitutively expressed in most kind of cells, we assumed that the results is more meaningful if we could obtain a difference between LGR5-overexpressing cells compared to the control empty vector cells, even though it is marginal. Moreover, we observed that parental KYN-2 cells had already reached the stage of anchorage-independent growth, while, a high level of LGR5 expression enhanced colony formation. This could be explained by high levels of LGR5 conferring resistance to cell death, and enhancing cell survival when they were scattered as single cells in the soft agar medium. KY-G1 cells aggregated and stacked up when cultured on the surface of the dishes, which consequently made them migrated slower than KY-V2 cells. These findings may explain why HCC is generally resistant to antitumor drugs used in chemotherapy. Many proteins related to the Wnt signaling pathway have been reported to modulate the actin–cytoskeleton structure. The frizzled/disheveled pathway controls the planar polarity of cells. Adenomatous polyposis coli (APC) protein is transported along microtubules, and regulates the cytoskeleton and cell migration [19]. β-catenin, a crucial transcription factor in the Wnt pathway, links E-cadherin with α-catenin to form firm adhesive junctions. LGR5, which is regarded as a target gene of the Wnt signaling pathway, quite possibly contributes to changes in cell morphology. Down-regulation of LGR5 in HepG2 and PLC/PRF/5 cells resulted in the cells acquiring a flat shape, with loss of cortical actin and migration of cells away from the aggregates. It also transformed HCC cells into a loosely associated morphology and increased cell motility. Reversely, high levels of LGR5 expression cells formed spherical shapes where most of the cells gathered intactly to the center. These results suggest that high levels of LGR5 expression affect epithelial cell morphology and confer some of the properties of stem cells on tumor cells.

To investigate the function of LGR5 in vivo, KY-G1 cells were orthotopically transplanted into NOG mice. KY-G1 cells formed nodular tumors typical of hepatocellular carcinomas, whereas the tumors formed by KY-V2 cells were diffuse and occasionally infiltrated into the contiguous tissues. Moreover, KY-V2 cells formed more micrometastases in the liver when implanted into the subcapsular region of the spleen. We previously categorized HCC cell lines into two groups; one highly metastatic and the

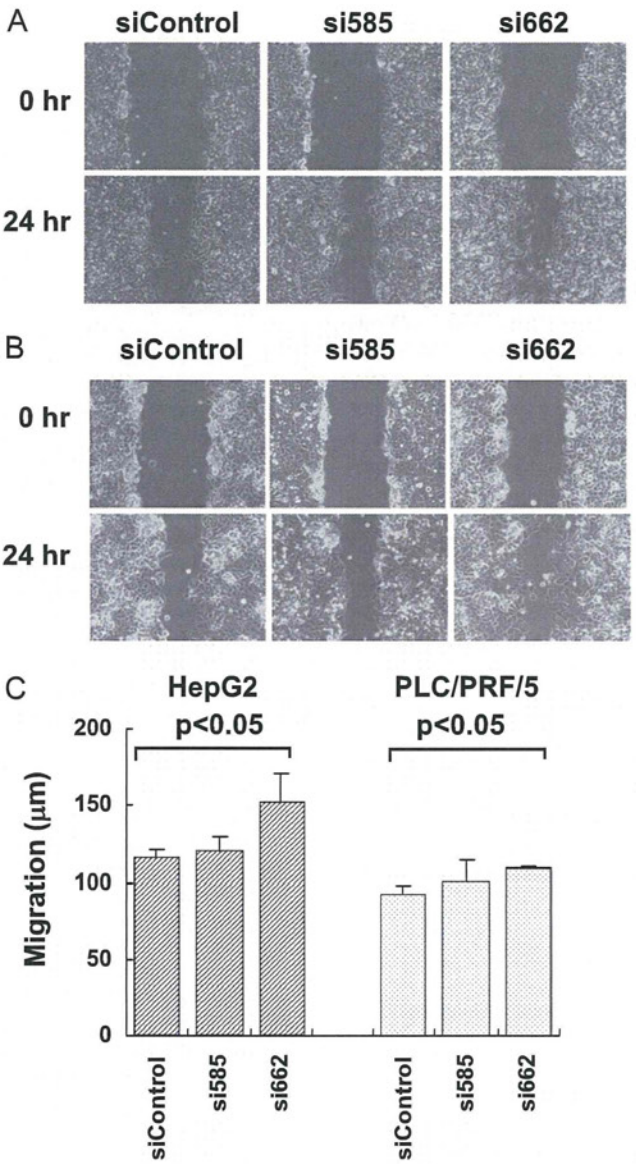

Fig. 5 – Motility of HCC cells after down-regulation of LGR5. Cells transfected with siControl, si585, or si662 were cultured for 2 days. Cell monolayers were scratched and photographed at 24 h. A: HepG2. B: PLC/PRF/5. C: Migration distance.

other non-metastatic [20]. It is quite interesting that KYN-2 and Li7 which express low levels of LGR5 were categorized as highly metastatic, whereas HepG2 and PLC/PRF/5 which express high levels of LGR5 were categorized in the non-metastatic group. Our previous clinicopathological study also showed that overexpression of LGR5 was more frequent in HCC with well to moderate differentiation compared with poorly differentiated HCC, although the difference was not statistically significant [6]. Here, we showed that the level of LGR5 expression in HCC cells affected the morphology of the tumors and their metastatic properties. Our present findings showed similar analogies with the features of clinical HCC regarding LGR5 expression. There is a possibility that high levels of LGR5 expression in HCC be the cause of the typical morphological and biological characteristics of some subclasses of HCC.

We observed similar morphological changes from various kinds of tumor cells by overexpression or down-regulation of LGR5 (unpublished data). One recent report showed that suppression of LGR5 expression in colorectal cancer cells enhanced tumor formation with increased cell motility, while cells overexpressing LGR5 tend to grow in 'colonies' with tight cell-to-cells contact and had reduction in cell motility [10]. Their observations on morphological changes and some other biological functions of LGR5 are mostly in agreement with our results, although the background of cell linage is different. Therefore, we think that our observations from the present study are not specific only to HCC, but are more generally applicable to the certain types of tumors.

Since the ligand of LGR5 has long been unknown, LGR5 has been categorized as an orphan receptor. Recently, R-spondins (Roof plate-specific Spondin, RSPOs) has been reported as ligands of LGR5 and required for sufficient activation of Wnt/β-catenin signaling [11,12,14]. To know whether overexpression of LGR5 affects the expression of RSPOs and potentiate Wnt/β-catenin signaling, we additionally measured expression of R-Spondin 1 (RSPO1) mRNA, and analyzed Wnt/β-catenin signaling level with

TOPflash/FOPflash TCF-luciferase reporter system (Supplementary Fig. 3). The expression of RSPO1 was not dependent on or related to in parallel with LGR5 expression. In HCC cell lines with high levels of LGR5 expression (HepG2), a high expression level of RSPO1 was observed. However, RSPO1 was also highly expressed in KIM 1 with low levels of LGR5. Also in LGR5-overexpressing cell (KY-G1, KY-S1) and empty vector cell (KY-V2, KY-V3), the expression of RSPO1 was not affected. In colorectal cell lines, expression level of RSPO1 was low in high LGR5 expressed cells, LoVo, whereas it was high in low expressed LGR5 cells, HCT116. We found that TOPFLASH/FOPFLASH ratio in LGR5-overexpressing KY-G1 cells was not significantly different from the vector-transfected clone. Furthermore, nuclear accumulation of β-catenin which is usually accompanied with activated Wnt signaling pathway was not detected in the LGR5-overexpressing clone (Fig. 1H). These results suggest that morphological changes and some other properties given from aberrant expression of LGR5 in tumor cells are not likely regulated by augmented Wnt signaling through R-spondin/LGR5 signaling pathway.

In this study we have shown that high levels of LGR5 expression confer cells with some of the properties of stem cells, including sphere formation and enhanced survival. In addition, high levels of LGR5 expression in vivo transformed tumors from a diffuse to a more nodular phenotype and from a metastatic to a less metastatic phenotype. These rather complicated biological roles of LGR5 may explain some of the complexity of human cancers, and further detailed studies of LGR5 would shed light on its biological functions and on the development of effective treatment strategies for cancer.

Disclosure statement

The authors have no conflict of interest.

Acknowledgments

We thank H. Suzuki, Y. Hashimoto and H. Abe for their excellent technical assistance. This work was supported by a Grant-in-Aid for Scientific Research (B) from the Ministry of Education, Culture, Sports, Science and Technology of Japan; and Third Term Comprehensive 10-Years Strategy for Cancer Control from the Ministry of Health, Labor and Welfare of Japan to M.S.

Appendix A. Supporting information

Supplementary data associated with this article can be found in the online version at http://dx.doi.org/10.1016/j.yexcr.2012.10.011.

REFERENCES

[1] H. Morita, S. Mazerbourg, D.M. Bouley, C.W. Luo, K. Kawamura, Y. Kuwabara, H. Baribault, H. Tian, A.J. Hsueh, Neonatal lethality of LGR5 null mice is associated with ankyloglossia and gastrointestinal distension, Mol. Cell. Biol. 24 (2004) 9736–9743.

[2] M.I. Garcia, M. Ghiani, A. Lefort, F. Libert, S. Strollo, G. Vassart, LGR5 deficiency deregulates Wnt signaling and leads to precocious Paneth cell differentiation in the fetal intestine, Dev. Biol. 331 (2009) 58–67.

[3] N. Barker, J.H. van Es, J. Kuipers, P. Kujala, M. van den Born, M. Cozijnsen, A. Haegebarth, J. Korving, H. Begthel, P.J. Peters, H. Clevers, Identification of stem cells in small intestine and colon by marker gene Lgr5, Nature 449 (2007) 1003–1007.

[4] N. Barker, R.A. Ridgway, J.H. van Es, M. van de Wetering, H. Begthel, M. van den Born, E. Danenberg, A.R. Clarke, O.J. Sansom, H. Clevers, Crypt stem cells as the cells-of-origin of intestinal cancer, Nature 457 (2009) 608–611.

[5] V. Jaks, N. Barker, M. Kasper, J.H. van Es, H.J. Snippert, H. Clevers, R. Toftgard, Lgr5 marks cycling, yet long-lived, hair follicle stem cells, Nat. Genet. 40 (2008) 1291–1299.

[6] Y. Yamamoto, M. Sakamoto, G. Fujii, H. Tsuiji, K. Kenetaka, M. Asaka, S. Hirohashi, Overexpression of orphan G-protein-coupled receptor, Gpr49, in human hepatocellular carcinomas with beta-catenin mutations, Hepatology 37 (2003) 528–533.

[7] K. Tanese, M. Fukuma, T. Yamada, T. Mori, T. Yoshikawa, W. Watanabe, A. Ishiko, M. Amagai, T. Nishikawa, M. Sakamoto, G-protein-coupled receptor GPR49 is up-regulated in basal cell carcinoma and promotes cell proliferation and tumor formation, Am. J. Pathol. 173 (2008) 835–843.

[8] T. McClanahan, S. Koseoglu, K. Smith, J. Grein, E. Gustafson, S. Black, P. Kirschmeier, A.A. Samatar, Identification of overexpression of orphan G protein-coupled receptor GPR49 in human colon and ovarian primary tumors, Cancer Biol. Ther. 5 (2006) 419–426.

[9] H. Uchida, K. Yamazaki, M. Fukuma, T. Yamada, T. Hayashida, H. Hasegawa, M. Kitajima, Y. Kitagawa, M. Sakamoto, Over-expression of leucine-rich repeat-containing G protein-coupled receptor 5 in colorectal cancer. Cancer Science 101 (2010) 1731–1737.

[10] F. Walker, H.H. Zhang, A. Odorizzi, A.W. Burgess, LGR5 is a negative regulator of tumourigenicity, antagonizes Wnt signalling and regulates cell adhesion in colorectal cancer cell lines. PloS one 6 (2011) e22733.

[11] W. de Lau, N. Barker, T.Y. Low, B.K. Koo, V.S. Li, H. Teunissen, P. Kujala, A. Haegebarth, P.J. Peters, M. van de Wetering, D.E. Stange, J.E. van Es, D. Guardavaccaro, R.B. Schasfoort, Y. Mohri, K. Nishimori, S. Mohammed, A.J. Heck, H. Clevers, Lgr5 homologues associate with Wnt receptors and mediate R-spondin signalling. Nature 476 (2011) 293–297.

[12] K.S. Carmon, Q. Lin, X. Gong, A. Thomas, Q. Liu, LGR5 interacts and cointernalizes with Wnt receptors to modulate Wnt/beta-catenin signaling. Molecular and Cellular Biology 32 (2012) 2054–2064.

[13] Y. Komiya, R. Habas, Wnt signal transduction pathways, Organogenesis 4 (2008) 68–75.

[14] A. Glinka, C. Dolde, N. Kirsch, Y.L. Huang, O. Kazanskaya, D. Ingelfinger, M. Boutros, C.M. Cruciat, C. Niehrs, LGR4 and LGR5 are R-spondin receptors mediating Wnt/beta-catenin and Wnt/PCP signalling. EMBO Reports 12 (2011) 1055–1061.

[15] T. Reya, S.J. Morrison, M.F. Clarke, I.L. Weissman, Stem cells, cancer, and cancer stem cells, Nature 414 (2001) 105–111.

[16] R. Pardal, M.F. Clarke, S.J. Morrison, Applying the principles of stem-cell biology to cancer, Nature Rev. 3 (2003) 895–902.

[17] N. Sato, L. Meijer, L. Skaltsounis, P. Greengard, A.H. Brivanlou, Maintenance of pluripotency in human and mouse embryonic stem cells through activation of Wnt signaling by a pharmacological GSK-3-specific inhibitor, Nature Med. 10 (2004) 55–63.

[18] X. Gong, K.S. Carmon, Q. Lin, A. Thomas, J. Yi, Q. Liu, LGR6 is a high affinity receptor of R-spondins and potentially functions as a tumor suppressor. PloS one 7 (2012) e37137.

[19] Y. Mimori-Kiyosue, C. Matsui, H. Sasaki, S. Tsukita, Adenomatous polyposis coli (APC) protein regulates epithelial cell migration and morphogenesis via PDZ domain-based interactions with plasma membranes, Genes Cells 12 (2007) 219–233.

[20] M. Chuma, M. Sakamoto, J. Yasuda, G. Fujii, K. Nakanishi, A. Tsuchiya, T. Ohta, M. Asaka, S. Hirohashi, Overexpression of cortactin is involved in motility and metastasis of hepatocellular carcinoma, J. hepatology 41 (2004) 629–636.

Hepatology Research

Hepatology Research 2013; 43: 35–43 doi: 10.1111/j.1872-034X.2012.01056.x

Special Report

A multicenter survey of re-treatment with pegylated interferon plus ribavirin combination therapy for patients with chronic hepatitis C in Japan

Tsugiko Oze,[1] Naoki Hiramatsu,[1] Eiji Mita,[3] Norio Akuta,[4] Naoya Sakamoto,[5] Hiroaki Nagano,[2] Yoshito Itoh,[7] Shuichi Kaneko,[8] Namiki Izumi,[6] Hideyuki Nomura,[9] Norio Hayashi[10] and Tetsuo Takehara[1]

Departments of [1]Gastroenterology and Hepatology and [2]Surgery, Osaka University Graduate School of Medicine, [3]National Hospital Organization Osaka National Hospital, Osaka, [4]Toranomon Hospital, [5]Department of Gastroenterology and Hepatology, Tokyo Medical and Dental University, [6]Japanese Red Cross Musashino Hospital, Tokyo, [7]Molecular Gastroenterology and Hepatology, Kyoto Prefectural University of Medicine Graduate School of Medical Science, Kyoto, [8]Department of Gastroenterology, Kanazawa University, Kanazawa, [9]Shin Kokura Hospital, Kitakyushu, and [10]Kansai Rosai Hospital, Amagasaki, Japan

Aim: This study aimed to clarify the factors associated the efficacy of re-treatment with pegylated interferon (PEG IFN) plus ribavirin combination therapy for patients with chronic hepatitis C who had failed to respond to previous treatment.

Methods: One hundred and forty-three patients who had previously shown relapse ($n = 79$), non-response ($n = 34$) or intolerance ($n = 30$) to PEG IFN plus ribavirin were re-treated with PEG IFN plus ribavirin.

Results: Twenty-five patients with intolerance to previous treatment completed re-treatment and the sustained virological response (SVR) rates were 55% and 80% for hepatitis C virus (HCV) genotype 1 and 2, respectively. On re-treatment of the 113 patients who completed the previous treatment, the SVR rates were 48% and 63% for genotype 1 and 2, respectively. Relapse after previous treatment and a low baseline HCV RNA level on re-treatment were associated with SVR in genotype 1 ($P < 0.001$). Patients with the interleukin-28B major genotype responded significantly better and earlier to re-treatment, but the difference in the SVR rate did not reach a significant level between the major and minor genotypes ($P = 0.09$). Extended treatment of 72 weeks raised the SVR rate among the patients who attained complete early virological response but not rapid virological response with re-treatment (72 weeks, 73%, 16/22, vs 48 weeks, 38%, 5/13, $P < 0.05$).

Conclusion: Relapse after previous treatment and a low baseline HCV RNA level have predictive values for a favorable response of PEG IFN plus ribavirin re-treatment for HCV genotype 1 patients. Re-treatment for 72 weeks may lead to clinical improvement for genotype 1 patients with complete early virological response and without rapid virological response on re-treatment.

Key words: chronic hepatitis C, pegylated interferon and ribavirin combination therapy, re-treatment

INTRODUCTION

PEGYLATED INTERFERON (PEG IFN) plus ribavirin combination therapy can show antiviral efficacy for patients with chronic hepatitis C (CH-C). However, a sustained virological response (SVR), which is defined as undetectable serum hepatitis C virus (HCV) RNA at 24 weeks after the treatment, remains at 50% for patients with HCV genotype 1 and 80% for those with HCV genotype 2 treated with PEG IFN plus ribavirin.[1–6] The number of patients who fail to achieve a SVR increases over time, requiring urgent action to eradicate HCV in them.

Recently, addition of the first-wave protease inhibitor telaprevir to PEG IFN plus ribavirin combination therapy, which has been reported to improve antiviral efficacy, has become commercially available, but this

Correspondence: Dr Tetsuo Takehara, Department of Gastroenterology and Hepatology, Osaka University Graduate School of Medicine, 2-2, Yamadaoka, Suita City, Osaka 565-0871, Japan. Email: takehara@gh.med.osaka-u.ac.jp

Received 18 April 2012; revision 19 May 2012; accepted 21 May 2012.

triple therapy increases side-effects, especially severe anemia and skin rash.[7–11] Second-wave protease inhibitors, such as TMC435, which not only improve antiviral efficacy but also decrease side-effects, have been developed and are undergoing clinical trials.[12] Also, IFN-free regimens, such as protease inhibitor and polymerase inhibitor combination therapy, have been developed.[13,14] In Japan, HCV carriers are increasing in an aging population, and large numbers of patients are ineligible for triple therapy with telaprevir due to potential anemia. That is why re-treatment with PEG IFN plus ribavirin is a possible choice for patients who failed to achieve SVR to previous antiviral therapy or patients ineligible for triple therapy with telaprevir who must wait until next-generation antiviral therapies, such as triple therapy with second-wave protease inhibitors or IFN-free regimens, become commercially available.

As for re-treatment with PEG IFN plus ribavirin, some studies have been reported but the subjects and treatment protocols were varied.[15–20] According to past reports, the previous treatment response is associated with the efficacy of the re-treatment[17,20] and the SVR rates in re-treatment ranged 4–23%.[16–18] Recently, host factors, such as single nucleotide polymorphisms (SNP) located near the interleukin (IL)-28B gene, and virus factors, such as the amino acid substitutions in the HCV core region, were revealed to have a strong impact on SVR in PEG IFN plus ribavirin combination therapy for naïve CH-C patients.[21–26] Moreover, response-guided therapy which extends treatment duration until 72 weeks for patients with a slow virological response can raise the SVR rate for naïve CH-C patients.[27–29] However, the value of IL-28B SNP has been uncertain in re-treatment and the most appropriate treatment duration in re-treatment is still unclear. Although it remains obscure which factors are associated with SVR in re-treatment with standard PEG IFN plus ribavirin therapy as pointed out above, some patients do respond to re-treatment and it is very important to be able to identify them. Such findings will be valuable for optimizing the antiviral treatment for CH-C patients by making it possible to decide which patients should be considered for re-treatment with PEG IFN plus ribavirin therapy and which should wait for next-generation antiviral treatment.

In the present study, we tried to determine which patients could benefit from re-treatment and to identify the factors associated with SVR in re-treatment, including the host genome SNP and treatment duration.

METHODS

Patients

THIS RETROSPECTIVE, MULTICENTER study was conducted by the Study Group of Antiviral Therapy for Difficult-to-Treat Chronic Hepatitis C supported by the Ministry of Health, Labor and Welfare, Japan. This study was conducted with 143 CH-C patients, 113 patients (genotype 1, $n = 86$; genotype 2, $n = 27$) who had previously completed PEG IFN-α-2b plus ribavirin combination therapy but had failed to attain SVR, and 30 patients (genotype 1, $n = 22$; genotype 2, $n = 8$) who had previously discontinued this combination therapy due to adverse events.

Treatment

For the previous treatment, patients had been treated with PEG IFN-α-2b (PEGINTRON; MSD, Whitehouse Station, NJ, USA) plus ribavirin (REBETOL; MSD). For re-treatment with PEG IFN plus ribavirin, patients were treated PEG IFN-α-2a (PEGASYS; Roche, Basel, Switzerland) plus ribavirin (COPEGUS; Roche) or PEG IFN-α-2b plus ribavirin. In principle, as a starting dose, PEG IFN was given once weekly at a dose of 180 μg of PEG IFN-α-2a and 1.5 μg/kg of PEG IFN-α-2b and ribavirin was given at a total dose of 600–1000 mg/day based on bodyweight (bodyweight, ≤60 kg, 600 mg; 60–80 kg, 800 mg; ≥80 kg, 1000 mg), according to the standard treatment protocol for Japanese patients and the decision of the investigator at the participating clinical center. Dose modification followed, as a rule, the manufacturer's drug information on the intensity of the hematological adverse effects.

Laboratory tests and virological assessment

Examination of peripheral blood, transaminase and the serum HCV RNA level were tested at the start of treatment, weeks 4, 12 and 24, end of treatment (EOT), and 24 weeks after the treatment. Sequences of the IFN-sensitivity determining region (ISDR) and the core region of HCV were determined at start of the previous treatment, and the number of mutations in the ISDR, the amino acid substitutions at core 70 and 91, glutamine (Gln) or histidine (His) at core 70 and methionine (Met) at core 91, were analyzed. Genetic polymorphisms located near the IL-28B gene (rs8099917) and ITPA gene (rs1127354) were determined. As for the IL-28B gene, homozygosity for the major sequence (TT) was defined as having the IL-28B major allele, whereas homozygosity (GG) or heterozygosity (TG) of the minor sequence was defined as having

the IL-28B minor allele. As for the ITPA gene, homozygosity for the major sequence (CC) was defined as having the ITPA major allele, whereas homozygosity (AA) or heterozygosity (CA) of the minor sequence was defined as having the ITPA minor allele. The serum HCV RNA level was quantified using the COBAS AMPLICOR HCV MONITOR test ver. 2.0 (detection range, 6–5000 KIU/mL; Roche Diagnostics, Branchburg, NJ, USA) or COBAS TaqMan HCV test (detection range, 1.2–7.8 $\log_{10}$ IU/mL) and qualitatively analyzed using the COBAS AMPLICOR HCV test ver. 2.0 (lower limit of detection, 50 IU/mL). When the serum HCV RNA level quantified by the COBAS TaqMan HCV test was less than 1.7 $\log_{10}$ IU/mL, which was equivalent to 50 IU/mL of HCV RNA, that case was judged as HCV RNA negativiation against the lower limit of detection of the COBAS AMPLICOR HCV test.

Definition of virological response

A rapid virological response (RVR) was defined as undetectable serum HCV RNA level at week 4, partial early virological response (p-EVR) as a more than 2-log decrease in the HCV RNA level at week 12 compared with the baseline, complete EVR (c-EVR) as undetectable serum HCV RNA at week 12, late virological response (LVR) as detectable serum HCV RNA at week 12 and undetectable at week 24, and SVR as undetectable serum HCV RNA at 24 weeks after the treatment. Relapse was defined as undetectable serum HCV RNA at the EOT but a detectable amount after the treatment. Patients without p-EVR or without clearance of HCV RNA at week 24 were considered to be showing non-response (NR), and treatment was stopped in both the previous treatment and this re-treatment. A patient who attained HCV RNA negativiation during the re-treatment continued to be treated for 48 weeks or 72 weeks according to response-guided therapy or the decision of the investigator at the participating clinical center.

Statistical analysis

Baseline data of the patients are expressed as means ± standard deviation or median values. In order to analyze the difference between baseline data or the factors associated with SVR, univariate analysis using the Mann–Whitney *U*-test or χ^2-test and multivariate analysis using logistic regression analysis were performed. A two-tailed *P*-value of less than 0.05 was considered significant. The analysis was conducted with SPSS ver. 17.0J (IBM, Armonk, NY, USA).

RESULTS

THE PATIENT FLOW in this study is shown in Figure 1. Among the patients who had previously discontinued PEG IFN-α-2b plus ribavirin combination therapy, two patients underwent splenectomy to increase platelet count prior to re-treatment, 25 completed re-treatment of PEG IFN plus ribavirin combination therapy and 15 achieved SVR (genotype 1, $n = 11$; genotype 2, $n = 4$).

All of the patients who completed previous treatment also completed re-treatment and the baseline characteristics of those patients are shown in Table 1. Of the 86 genotype 1 patients, 54 were relapsers and 32 had shown NR to previous treatment. Of the 27 patients with genotype 2, 25 were relapsers and two had shown NR to previous treatment. Thirty-seven patients with genotype 1 and 14 patients with genotype 2 were assessed as IL-28B genotype, and 27 patients with genotype 1 and 10 patients with genotype 2 were assessed as ITPA genotype. There was no significant difference in the baseline characteristics between the previous treatment and the re-treatment with respect to peripheral blood cell counts, amino transaminase level and serum HCV RNA at the start of treatment (Table 1).

The baseline characteristics of patients with genotype 1 according to antiviral efficacy of the previous treatment are shown in Table 2. Among those with NR in the previous treatment, the rate of the minor allele of IL-28B was significantly higher than those with relapse in the previous treatment ($P < 0.01$). For genotype 1, the HCV RNA negative rate on re-treatment was 20% (17/86) at week 4, 61% (52/85) at week 12 and 76% (65/86) at week 24, and the SVR rate was 48% (41/86). The factors associated with SVR were assessed by univariate analysis and the factors of relapse after previous treatment and the serum HCV RNA level at the start of re-treatment were selected as being significant (Table 3). The SVR

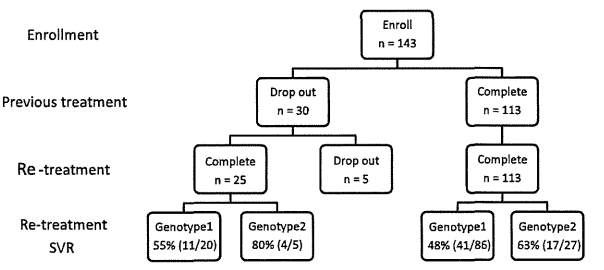

Figure 1 Patient flow for this study. SVR, sustained virological response.

Table 1 Baseline characteristics of patients and treatment factors in previous treatment and re-treatment

Factor	Genotype 1		Genotype 2	
No.	86		27	
Sex: male/female	46/40		15/12	
Effect of previous treatment: relapse/NR	54/32		25/2	
	Previous treatment	Re-treatment	Previous treatment	Re-treatment
PEG IFN type: α-2a/α-2b	0/86	41/45	0/27	6/21
Age (years)	58.1 ± 8.3	60.0 ± 8.5	58.9 ± 8.2	60.0 ± 8.1
White blood cells (/mm^3)	4779 ± 1383	4610 ± 1443	5195 ± 1473	4724 ± 1266
Neutrophils (/mm^3)	2478 ± 930	2355 ± 1071	2561 ± 827	2389 ± 941
Hemoglobin (g/dL)	13.7 ± 1.2	13.5 ± 1.7	14.4 ± 1.3	14.0 ± 1.2
Platelets (×10^4/mm^3)	16.0 ± 5.9	16.6 ± 6.2	18.0 ± 5.7	16.8 ± 5.2
ALT (IU/L)	75 ± 51	73 ± 72	57 ± 46	42 ± 32
Histology: activity, 0–1/2–3	29/29		11/7	
Fibrosis, 0–2/3–4	45/14		17/1	
Serum HCV RNA (KIU/mL)	1600	850	1500	700
IL-28B SNP: rs8099917; TT/TG	26/11		10/4	
ITPA SNP: rs1127354; CC/CA	20/7		9/1	
Core 70: wild/mutant	11/11			
Core 91: wild/mutant	15/7			
ISDR: 0–1/≥2	15/1			

ALT, alanine aminotransferase; HCV, hepatitis C virus; IFN, interferon; IL, interleukin; ISDR, IFN-sensitivity determining region; NR, non-response; PEG, pegylated; SNP, single nucleotide polymorphism.

rates of relapsers were significantly higher than those of patients with NR in the previous treatment (relapse, 67%, 36/54 vs NR, 16%, 5/32, $P < 0.0001$). As for the serum HCV RNA level at the start of re-treatment, although the SVR rate of those patients with 5 $\log_{10}$ IU/mL or more of HCV RNA was 38% (26/69), all patients with less than 5 $\log_{10}$ IU/mL of HCV RNA attained SVR (11/11) ($P = 0.0001$). As for the IL-28B genotype, among the patients with the major allele, the p-EVR rate was significantly higher and the EOT response rate showed marginal significance compared to that with the minor allele (p-EVR rate, 100%, 23/23 vs 30%, 3/10, $P < 0.0001$, EOT rate, 92%, 24/26 vs 64%, 7/11, $P = 0.05$). There was no significant difference of the SVR rate between major and minor alleles (major, 65%, 17/26 vs minor, 36%, 4/11, $P = 0.15$).

Figure 2(a) shows the result of stratified analysis according to the previous treatment response and HCV RNA at the start of re-treatment. The significant difference in SVR observed between high (≥5 $\log_{10}$ IU/mL) and low (<5 $\log_{10}$ IU/mL) baseline viral loads was still found in both previous relapsers ($P = 0.02$) and previous non-responders ($P = 0.02$). In patients with a high baseline viral load, previous relapsers achieved a higher SVR rate than previous non-responders ($P < 0.0001$). Next, the results of stratified analyses according to IL-28B genotype and previous treatment response or HCV RNA at the start of re-treatment showed no significant difference in SVR rates between the IL-28B genotype in patients with relapse after previous treatment ($P = 0.63$) (Fig. 2b). All patients with less than 5 $\log_{10}$ IU/mL of HCV RNA achieved SVR despite their IL-28B genotype and the SVR rates of patients with 5 $\log_{10}$ IU/mL or more of HCV RNA did not differ between IL-28B genotypes (Fig. 2c). Multivariate analysis among the factors of relapse to previous treatment response, HCV RNA at the start of re-treatment and IL-28B genotype showed that relapse after previous treatment response bore the most predictable relationship to SVR in re-treatment ($P = 0.074$).

As for the efficacy of re-treatment according to treatment duration among patients with HCV RNA negativity during re-treatment, the SVR rate of 72-week treatment was significantly higher than that of 48-week treatment (72 weeks, 73%, 29/40, vs 48 weeks, 52%, 12/25, $P < 0.05$). This significant difference was especially found in patients who attained c-EVR but not RVR on re-treatment (72 weeks, 73%, 16/22, vs 48 weeks,

Table 2 Baseline characteristics of patients and treatment factors according to the virological response in previous treatment among patients with genotype 1

Factor	Relapser in previous treatment		NR in previous treatment	
No.	54		32	
Sex: male/female	28/26		18/14	
	Previous treatment	Re-treatment	Previous treatment	Re-treatment
PEG IFN type: α-2a/α-2b	0/54	29/25	0/32	12/20
Age (years)	58.1 ± 8.1	60.3 ± 8.4	57.9 ± 8.9	59.6 ± 8.8
White blood cells (/mm^3)	4917 ± 1290	4692 ± 1035	4546 ± 1520	4462 ± 1993
Neutrophils (/mm^3)	2618 ± 846	2479 ± 805	2225 ± 1033	2105 ± 1454
Hemoglobin (g/dL)	13.9 ± 1.2	13.7 ± 1.6	13.5 ± 1.3	13.1 ± 1.9
Platelets (×10^4/mm^3)	17.1 ± 6.3	17.7 ± 6.1	14.1 ± 4.7	14.7 ± 6.2
ALT (IU/L)	75 ± 57	70 ± 76	75 ± 39	78 ± 64
Histology: activity, 0–1/2–3	20/18		9/11	
Fibrosis, 0–2/3–4	31/8		14/6	
Serum HCV RNA (KIU/mL)	1600	980	1550	800
IL-28B SNP: rs8099917; TT/TG	24/5		2/6	
ITPA SNP: rs1127354; CC/CA	15/6		5/1	
Core 70: wild/mutant	6/6		5/5	
Core 91: wild/mutant	9/3		6/4	
ISDR: 0–1/≥2	9/0		6/1	

ALT, alanine aminotransferase; HCV, hepatitis C virus; IFN, interferon; IL, interleukin; ISDR, IFN-sensitivity determining region; NR, non-response; PEG, pegylated; SNP, single nucleotide polymorphism.

38%, 5/13, $P < 0.05$) but not in patients who attained RVR or LVR (Fig. 3).

In genotype 2, the HCV RNA negative rate on re-treatment was 59% (16/27) at week 4, 85% (23/27) at week 12 and 93% (25/27) at week 24, and the SVR rate was 63% (17/27). The two patients with NR in previous treatment did not attain SVR with re-treatment. The factors associated with SVR were assessed by univariate analysis and only the factor of younger age at the start of re-treatment showed marginal significance ($P = 0.06$) (Table 4). Among the patients with RVR on re-treatment, the SVR rates were similar at 75% (6/8) to those with 24-week and 48-week treatment.

DISCUSSION

PAST STUDIES HAVE revealed that the factors of age, sex, progression of liver fibrosis, value of HCV RNA, number of mutations in the ISDR, amino acid substitutions in the core region, drug adherence and treatment duration show association with HCV eradication in PEG IFN plus ribavirin combination for naïve patients with CH-C.[3–5,25–33] Recently, the IL-28B genotype has been reported to be the most powerful factor associated with the antiviral effect of this combination therapy.[21–25] While the predictive factors for SVR in PEG IFN plus ribavirin combination therapy for naïve patients have been actively analyzed, those factors for patients who had already experienced this therapy are still unclear. Especially needing assessment is the correlation between IL-28B SNP or the previous treatment response and the antiviral effect in re-treatment. In this study, we tried to determine which factors could most effectively predict the antiviral effect in re-treatment.

In the present study, patients with relapse after the previous treatment and patients with a low serum HCV RNA level at the start of re-treatment showed significantly different results in this study of re-treatment of CH-C patients who had previously failed to attain SVR with PEG IFN plus ribavirin therapy. This result was similar to those of the EPIC[3] study on relapse and NR[17] and the SYREN trial of NR.[18] On the other hand, there was no significant difference between the influence of the IL-28B genotype and SVR. More specifically, if the previous treatment response was the same, there was no difference regardless of the IL-28B genotype. Considering this result, in re-treatment, the previous treatment response was a more effective predictive factor than IL-28B genotype. However, further investigation is needed to clarify the association between IL-28B

Table 3 Factors associated with a sustained virological response in re-treatment with PEG IFN plus ribavirin in patients with genotype 1

Factor		SVR	Non-SVR	*P*-value
No. of patients		41	45	
Age (years)		60.2 ± 7.1	59.9 ± 9.6	0.71
Sex: male/female		24/17	22/23	0.40
Serum HCV RNA (log IU/mL)		5.8 ± 1.4	6.4 ± 0.6	0.11
Serum HCV RNA: <5 log/≥5 log		11/28	0/43	<0.001
White blood cells (/mm^3)		4656 ± 1029	4566 ± 1763	0.42
Neutrophils (/mm^3)		2443 ± 804	2259 ± 1301	0.16
Hemoglobin (g/dL)		13.5 ± 1.6	13.4 ± 1.8	0.80
Platelets (×10^4/mm^3)		16.9 ± 5.7	16.3 ± 6.7	0.36
ALT (IU/L)		68 ± 69	78 ± 75	0.43
IL-28B SNP: TT/TG		17/4	9/7	0.15
ITPA SNP: CC/CA		13/3	7/4	0.39
Core 70: wild/mutant		5/4	6/7	1.00
Core 91: wild/mutant		7/3	8/5	1.00
ISDR: 0–1/≥2		9/0	6/1	0.44
PEG IFN: α-2a/α-2b		16/25	25/20	0.14
PEG IFN dose (μg/kg per week)	α-2a	2.91 ± 0.77	2.74 ± 0.69	0.61
	α-2b	1.25 ± 0.39	1.20 ± 0.32	0.59
Ribavirin dose (mg/kg per day)		9.34 ± 2.72	9.64 ± 3.20	0.51
1st treatment virological response	Relapse/NR	36/5	18/27	<0.001

ALT, alanine aminotransferase; HCV, hepatitis C virus; IFN, interferon; IL, interleukin; ISDR, IFN-sensitivity determining region; NR, non-response; PEG, pegylated; SNP, single nucleotide polymorphism; SVR, sustained virological response.

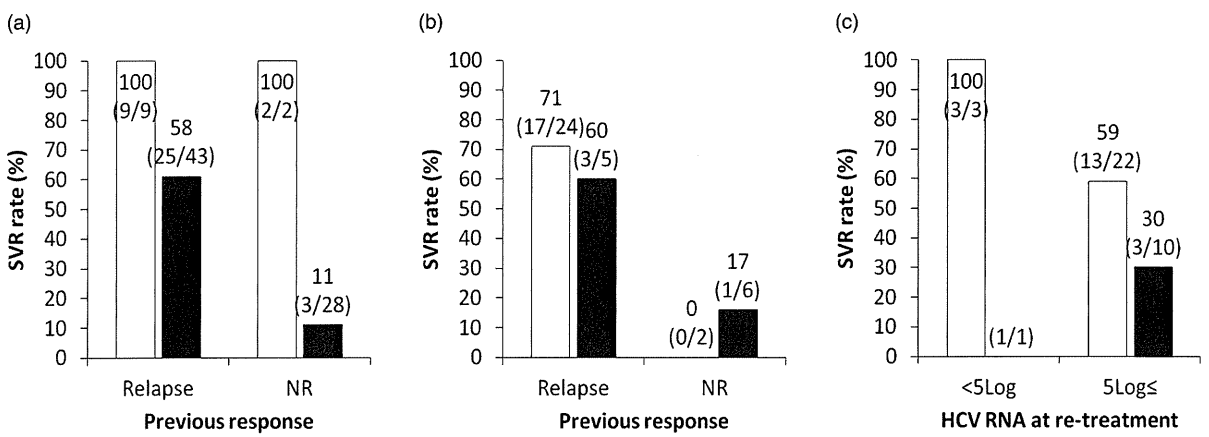

Figure 2 Sustained virological response (SVR) rates according to previous virological response, hepatitis C virus (HCV) RNA at start of re-treatment and genotype of interleukin (IL)-28B single nucleotide polymorphism (SNP) in patients with genotype 1. (a) Stratified analysis of previous virological response and HCV RNA at start of re-treatment. □, HCV RNA <5 log IU/mL at start of re-treatment; ■, HCV RNA ≥5 log IU/mL at start of re-treatment. (b) Stratified analysis of previous virological response and genotype of IL-28B SNP. □, Patients with major allele of IL-28B SNP; ■, patients with minor allele of IL-28B SNP. (c) Stratified analysis of HCV RNA at start of re-treatment and genotype of IL-28B SNP. □, Patients with major allele of IL28B SNP; ■, patients with minor allele of IL-28B SNP.